

Animation and Visualization of Spot Prices via Quadratized Power Flow Analysis

A. P. Sakis Meliopoulos, Sun Wook Kang
*School of Electrical Engineering and Computer
 Engineering*
Georgia Institute of Technology
Atlanta, Georgia 30332 – 0250
sakis.meliopoulos@ece.gatech.edu

G. J. Cokkinides, Roger Dougal
Department of Electrical Engineering
University of South Carolina
Columbia, SC 29208
cokkinides@attbi.com

Abstract

This paper presents a new model for efficient calculation of spot prices and animation and visualization of spot price evolution as the system operating point is changing. The computational method is based on the quadratized power flow approach that cast the power flow problem as a set of quadratic equations. The load model consists of constant power, constant impedance and induction motor loads. The electric load time variation is modeled via a small set of independent random variables resulting in a nonconforming electric load model. Constraints of voltage limits as well as circuit loading are imposed. For a specific load point, the operation of the system is determined by the appropriate formulation of the power flow problem and subsequent solution. At this operating point, the spot prices are computed from a linear program defined at the operating point. The results are visualized in a three-dimensional OpenGL display. As the system load evolves, the spot prices are recomputed and the visualization display is updated thus generating an animated evolution of the system spot prices. The paper describes the proposed computational method and discusses the efficiency of the proposed method. The method is also demonstrated on the IEEE RTS system which has been modified to include a model of a spot price market. The presentation of the paper will include a demonstration of the visualization and animation of the spot prices for the IEEE RTS system.

Keywords: *Spot Prices, power flow, linear program, visualization, animation.*

1. Introduction

Recent industry trends and formation of power markets have generated the requirement of better ways to understand the spot market or day ahead markets, or any other form of market structure. Independently of market structures, a better way of displaying and disseminating market relevant quantities has become a desirable tool. This paper is focused on providing a better model for the

computation of market relevant quantities and displaying these quantities in an animated fashion. We have selected spot prices as the market relevant quantities to be displayed. The proposed procedures are equally applicable to any other market relevant quantities.

A key component of the proposed approach is to develop a better model for the computation of spot prices. The proposed model consists of four innovations: (a) a quadratic power flow model, (b) a nonconforming electric load model, (c) an efficient linearization procedure based on the co-state method for setting-up a linear program for the computation of spot prices, and (d) a geometric construction of the three-dimensional display of spot prices for any system geography, implemented in OpenGL.

The paper describes the above four innovations. An example application is presented for a small electric power system. Snapshot displays of the animations are given in the paper. In addition, the IEEE RTS system [9] has been modified to include a spot market model. At the presentation of the paper, live demonstration of the animations will be given.

2. Proposed Power Flow Model

We present a new power flow formulation where the electric load is assumed to consist of any combination of (a) constant power load, (b) constant impedance load, (c) induction motor load, and (d) switched shunt capacitors or reactors. The usual power flow assumptions are also made i.e. the system operates under balanced conditions and the system components are represented by their positive sequence models.

Figure 1 shows a symbolic representation of a general power system bus. A generator, a constant impedance load, a constant power load, an induction motor load, and switched shunt capacitor/reactors are connected to the bus together with a transformer and a circuit (transmission line) to other buses. As an example, the

generator and circuit models are described next. The generator model is nonlinear and the circuit model is linear.

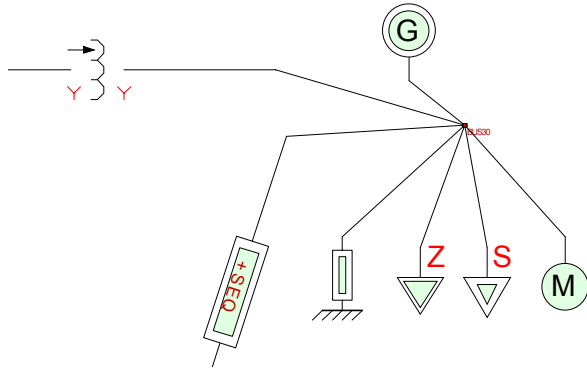


Figure 1. Symbolic Representation of a General Power System Bus – Positive Sequence Network

Generator Model. The illustration below shows the mathematical model and icon used in the graphical user interface for the generator model.

Mathematical model	Icon

The generator has three control modes: (a) Slack mode (voltage magnitude and phase angle control), (b) real and reactive power control (PQ mode), and (c) real power and bus voltage magnitude control (PV mode). The equation representing each of these modes are given below.

Slack mode: This control mode sets the bus voltage magnitude to a specified value and the bus voltage phase to zero. The following equations hold:

$$\tilde{I}_{gk} = \frac{1}{3}(-P_{gk} + jQ_{gk}) \frac{1}{\tilde{V}_k^*} \quad (1)$$

$$0.0 = V_{ki}$$

$$0.0 = V_{kr}^2 + V_{ki}^2 - V_{k, \text{given}}^2$$

Where: The subscripts r and i indicate phasor real and imaginary parts, and the subscript k is the bus number where the generator is connected, $P_{gk} + jQ_{gk}$ is the complex power produced by the generator, and $V_{k, \text{given}}$ is the specified voltage magnitude

PQ mode: This control mode sets the real and reactive power injected into the bus to specified values. The following equations hold:

$$\tilde{I}_{gk} = \frac{1}{3}(-P_{gk} + jQ_{gk}) \frac{1}{\tilde{V}_k^*} \quad (2)$$

PV mode: This control mode sets the real power injected into the generator bus and bus voltage magnitude to specified values. The following equations hold:

$$\tilde{I}_{gk} = \frac{1}{3}(-P_{gk} + jQ_{gk}) \frac{1}{\tilde{V}_k^*} \quad (3)$$

$$0.0 = V_{kr}^2 + V_{ki}^2 - V_{k, \text{given}}^2$$

Note that the above equations are nonlinear with respect to the state variables.

Circuit Branch Model. The illustration below shows the mathematical model and icon of a circuit branch model.

Mathematical model	Icon

The circuit branch model is represented by the following equation:

$$\tilde{I}_k = (\tilde{y}_{km} + \tilde{y}_{skm})\tilde{V}_k - \tilde{y}_{km}\tilde{V}_m \quad (4)$$

$$\tilde{I}_m = -\tilde{y}_{km}\tilde{V}_k + (\tilde{y}_{km} + \tilde{y}_{smk})\tilde{V}_m$$

Where

\tilde{y}_{km} is the branch series admittance

\tilde{y}_{skm} is the k side branch shunt admittance

\tilde{y}_{smk} is the m side branch shunt admittance

\tilde{V}_k is the voltage phasor at bus k .

\tilde{V}_m is the voltage phasor at bus m .

Note that these equations are linear with respect to the state variables.

Note that each component of the system can be represented with an appropriate set of linear or quadratic equations.

Solution Method: The network solution is obtained with application of Newton's method to a quadratized form of the network equations. The quadratized network equations are generated as follows.

The equations of each nonlinear model are cast in the following form:

$$\begin{bmatrix} \tilde{I}^k \\ 0 \end{bmatrix} = y_{eq_cmpx}^k \begin{bmatrix} \tilde{V}^k \\ \tilde{Y}^k \end{bmatrix} + F \left\{ \begin{bmatrix} x^{kT} f_{eq_real1}^k x^k \\ x^{kT} f_{eq_real2}^k x^k \\ \vdots \end{bmatrix} \right\} - b_{eq_cmpx}^k \quad (5)$$

Where \tilde{I}^k : vector of bus current injections,

\tilde{V}^k : vector of bus voltages,

\tilde{Y}^k : vector of device internal state variables,

$$\tilde{X}^k = \begin{bmatrix} \tilde{V}^k & \tilde{Y}^k \end{bmatrix}^T,$$

x^k = vector \tilde{X}^k in cartesian Coordinates

and $y_{eq_cmpx}^k$, $b_{eq_cmpx}^k$, and $f_{eq_real}^k$ are matrices with appropriate dimensions. $F(\cdot)$ denotes a function mapping from a real vector to a complex vector. Note that this form includes two sets of equations, which are named *external equations* and *internal equations* respectively. The bus current injections appear only in the external equations. Similarly, the device states consist of two variable sets: *external states* (i.e. bus voltage phasors \tilde{V}^k) and *internal state variables* \tilde{Y}^k (if any). The set of equations (2) is consistent in the sense that the number of external states and the number of internal states equals the number of external and internal equations respectively.

The entire network equations are obtained by application of the connectivity constraints among the system component, i.e. Kirchoff's current law at each system bus. This procedure yields a set of equations, which are combined with the component object internal equations resulting in the set of equations of the form:

$$\sum_k A^k \tilde{I}^k = 0 \quad (6)$$

[plus internal equations of all devices]

where \tilde{I}^k is device k bus current injections, and A^k is a component incidence matrix with:

$$\begin{cases} \{A_{ij}^k\} = 1, & \text{if bus } j \text{ of device } k \text{ is connected to bus } i \\ & = 0, \text{ otherwise} \end{cases}$$

Let \tilde{V} be the vector of all bus voltage phasors. Then, the following relationship holds:

$$\tilde{V}^k = (A^k)^T \tilde{V} \quad (7)$$

where \tilde{V}^k is device k bus voltages. Upon substitution of device equations (5) and incidence equations (7), equation (6) becomes a set of quadratic equations:

$$\tilde{Y} \tilde{X} + F \begin{bmatrix} x^T f_1 x \\ x^T f_2 x \\ \vdots \end{bmatrix} - \tilde{B} = 0 \quad (8)$$

where \tilde{X} is the vector of all the state variables and \tilde{Y}, f, B are matrices with appropriate dimensions. The simultaneous solution of these equations is obtained via Newton's method described next.

The numerical algorithm for solving the network equations (8) consists of two steps. First, we convert the network equations into Cartesian coordinates by simply replacing each complex variable with its Cartesian form and separating the real and imaginary parts of the complex equations. The procedure is equivalent with replacing each element in \tilde{Y} with its corresponding 2×2 Hermetian matrix. In particular, \tilde{Y}_{ij} is replaced by:

$$\begin{bmatrix} \tilde{Y}_{ij}^r & -\tilde{Y}_{ij}^i \\ \tilde{Y}_{ij}^i & \tilde{Y}_{ij}^r \end{bmatrix} \quad (9)$$

where superscript r denotes real part and superscript i denotes imaginary part. Then, equation (8) is transformed into Equation (10) below:

$$Y_{real} x + \begin{bmatrix} x^T f_1 x \\ x^T f_2 x \\ \vdots \end{bmatrix} - B_{real} = 0 \quad (10)$$

Equation (7) is solved using Newton's method. Specifically, the solution is given by the following algorithm:

$$x^{v+1} = x^v - J^{-1} \left\{ Y_{real} x^v + \begin{bmatrix} x^{vT} f_1 x^v \\ x^{vT} f_2 x^v \\ \vdots \end{bmatrix} - B_{real} \right\} \quad (11)$$

where v is the iteration step number; J is the Jacobian matrix of equation (10). In particular, the Jacobian matrix takes the following form:

$$J = Y_{real} + \begin{bmatrix} x^{vT} (f_1 + f_1^T) \\ x^{vT} (f_2 + f_2^T) \\ \vdots \end{bmatrix} \quad (12)$$

It is important to note that Newton's method applied to a set of quadratic equations guarantees quadratic convergence. In fact, this algorithm (8) converges in only two to four iterations. The convergence speed for a specific case is illustrated in Table 1. The table gives the total mismatch vector norm (specifically the maximum absolute real and reactive power at all system buses) after each Newton's method iteration applied to the solution of a 15 bus system.

Iteration #	Maximum Mismatch
1	205
2	0.087
3	0.0094
4	0.00000091

3. Spot Price Computational Model

The spot prices are computed with a linearized model around an operating conditions. For this purpose, we utilize the linearization procedure based on the co-state method, an electric load model (conforming or not conforming) and a linear programming formulation. The constituent parts of the methodology are described next.

Electric Load Model: This model presents changes of electric load in terms of a single parameter (conforming load) or in terms of a small number of parameters (non-conforming load).

Conforming Load Model: The conforming electric load model allocates the total load to the individual buses via a linear relationship. The uncertainty is represented with a single random variable. The general expression of the bus loads is:

$$P_{bus}(t) = d(t)P_0 + \sigma(t)vP_1 \quad (13)$$

where:

$P_{bus}(t)$ is an n -vector of bus electric load,

n is the number of buses

$d(t)$ is the electric load forecast

$\sigma(t)$ is the standard deviation of the electric load forecast

P_0 is an n -vector for allocating an electric load to the n buses of the system (sum of entries equals 1.0)

P_1 is an n -vector for allocating an electric load to the n buses of the system (sum of entries equals 1.0)

v is a random variable.

Note that the above model is a simple model that extensively used by power system planners. It is presented here to illustrate that the model we plan to use (the non-conforming load model) is an extension of this model.

Non-Conforming Load Model: The non-conforming load model is an extension of the conforming load model. Specifically, with the introduction of additional random variables, the non-conforming load model is obtained. The non-conforming load model has the capability to represent the statistical correlation among the bus loads. It is expressed as follows:

$$P_{bus}(t) = d(t)P_0 + \sigma(t) \sum_{i=1}^m v_i P_i \quad (14)$$

where:

$P_{bus}(t)$ is an n -vector of bus electric load,

n is the number of buses

$d(t)$ is the electric load forecast

$\sigma(t)$ is the standard deviation of the electric load forecast

P_0 is an n -vector for allocating an electric load to the n buses of the system (sum of entries equals 1.0)

P_i is an n -vector for allocating an electric load to the n buses of the system (sum of entries equals 1.0), $i=1, 2, \dots, m$

v_i is a random variable, $i=1, 2, \dots, m$

Note that the proposed load model is expressed in terms of m random variables.

Linearized Model: This procedure derives a linearized model of the network operations around the present operating conditions. Consider a operating quantity, i.e. bus voltage magnitude, circuit flow, unit reactive power, etc. The operating quantity can be expressed as a function of the system state and controls. The controls are power injections into the nodes of the system. We represent this quantity as:

$$J = f(X, p) \quad (15)$$

$$p: S_{dk} = p_k(1 + ja_k), \quad \text{injection at bus } k.$$

The linearized model is obtained with the use of the co-state method [8]. This method yields the following.

$$\frac{dJ}{dp} = \frac{\partial f(X, p)}{\partial p} - \hat{x}^T \frac{\partial G(X, p)}{\partial p} \quad (16)$$

where:

$$\hat{x}^T = \left[\frac{\partial f(X, p)}{\partial X} \right] \left[\frac{\partial G(X, p)}{\partial X} \right]^{-1}$$

This method is very efficient as the only significant computational task is the computation of the co-state vector which can be accomplished with a forward and back substitution on the vector $\left[\frac{\partial f(X, p)}{\partial X} \right]$ with the known factors of the jacobian matrix.

Spot Price Computations: The spot prices are directly computed with an optimization problem of the linear programming variety. Specifically, the spot prices are defined with:

$$\text{Min } C = \sum p_i P_i \quad (17)$$

Subject to: - power flow equations
- operating constraints

Upon linearization of the operating constraints and elimination of the power flow equations using the co-state method, the following problem is emerged.

$$\text{Min } C = \sum p_i P_i \quad (18)$$

$$\begin{aligned} & Ay + BP + z = b + Db_d \\ \text{subject to: } & \sum P_i = b_d \end{aligned}$$

The spot price is defined by the following derivative at the optimum solution:

$$\text{Spot Price} = \frac{dC}{db_d} \quad (19)$$

Above derivative is directly computed from the dual linear programming problem. Specifically, the dual problem is:

$$\text{Max } M = \sum c_i \lambda_i \quad (20)$$

$$\text{subject to: } A' \lambda = p$$

The spot price is provided as a linear combination of the solution of the dual linear programming problem.

$$\text{Spot Price} = \frac{dC}{db_d} = e^T \lambda \quad (21)$$

Note that once the primal problem solution is known, then the solution of the dual problem is obtained by a simple solution of a set of linear equations. The reason for this is that we know the basic variables from the primal problem and therefore, there is no need to perform a full optimization algorithm. The primal solution is known, it is the present operating condition. These observations make the algorithm very fast.

4. Visualization of Spot Prices

Once the spot prices have been computed, they are displayed using 3-dimensional graphics. Specifically the spot prices are plotted within a 3-D environment. The single line-line diagram of the simulated network is displayed over a horizontal plane. The single line diagram can be drawn to scale, and additional geographic features may be optionally included. The spot price distribution over the geographical occupied by the simulated network is represented by a curved surface overlaying the single line diagram drawing. The height of the surface at a certain point represents the spot price at that point. Note that although the spot prices are computed only at discrete points (i.e. the system buses), a smooth and continuous spot price surface plot is

generated by interpolation. The curved surface is drawn in translucent mode so that the single line diagram and other geographic features can be seen through the spot price surface plot. Visualization is further enhanced by allowing perspective view rotation, zooming and panning.

Spot Price Animation. The effect of changing spot prices as the load changes can be visualized by animation of the above described spot price 3-D plot. As the user changes the electric load, the spot prices are automatically recomputed and the 3-D spot price plot is updated. Note that the graphic display implementation uses the OpenGL system, which provides very fast display refresh rates resulting in an animation effect.

Spot Price Visualization Example. The described visualization methodology is demonstrated with an example system. Figure 2 illustrates the single line diagram of the example system. It is a 14 bus system with 6 generating units. Figure 3 illustrates a snapshot of the spot price visualization display. The blue surface represents the spot prices. The system single line diagram can be seen through the spot price surface. The visualization software has complete zoom and pan capabilities and therefore is amenable to visualizations of larger systems. During the presentation of the paper, the method will be demonstrated on the 24 bus and 96 bus IEEE RTS system.

Conclusions

This paper has presented a new approach for the computation of spot prices in an electric power system and the animated display of spot prices as the electric load is changing. The proposed innovations are: (a) a quadratic power flow model, (b) a nonconforming electric load model, (c) an efficient linearization procedure based on the co-state method for setting-up a linear program for the computation of spot prices, and (d) a geometric construction of the three-dimensional display of spot prices for any system geography, implemented in OpenGL. The method is capable of representing electric loads that consist of constant power, constant impedance, induction motors, etc. The efficiency of the method permits the fast visualization and animation of spot prices. It is expected that this method will be extended to visualizations and animations of other market relevant quantities.

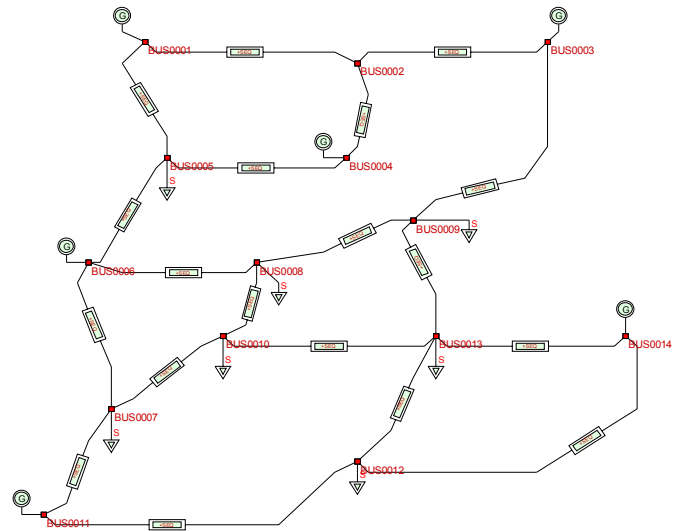


Figure 2. Example System for Spot Price Visualization

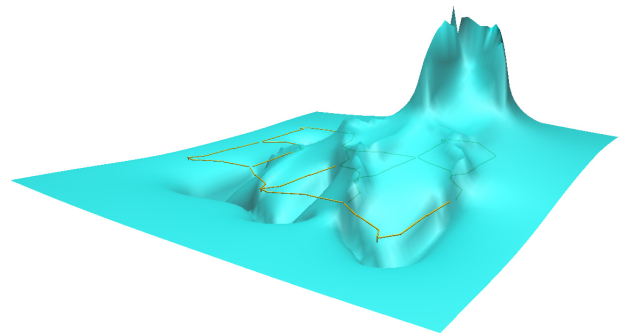


Figure 3. Spot Price 3-D Surface Plot

Acknowledgements

The work reported in this paper has been partially supported by the ONR Grant No. N00014-00-1-0131 and NSF/PSERC project E21-F96. This support is gratefully acknowledged.

References

1. A. P. Sakis Meliopoulos, *Comprehensive Power System Reliability Assessment*, Presentation for PSERC Reliability Research, July 2000.
2. E. Fitzgerald, Charles Kingsley, Jr., Stephen D. Umans, *Electric Machinery*, Fifth Edition, McGraw-Hill, Inc. 1990.
3. Turan Gonen, *Electrical Machines*, Power International Press, 1998.
4. John J. Grainger, William D. Stevenson, Jr., *Power System Analysis*, McGraw-Hill, Inc. International Editions 1994.

5. IEEE Task Force on Load Representation for Dynamic Performance, System Dynamic Performance Subcommittee, and Power System Engineering Committee, "Bibliography on load models for power flow and dynamic performance simulation", *IEEE Transactions on Power Systems*, Vol. 10, No. 1, PP. 523 –538, February 1995.
6. System Dynamic Performance Subcommittee and Power System Engineering Committee, "Standard load models for power flow and dynamic performance simulation", *IEEE Transactions on Power Systems*, Vol. 10, No. 3, PP. 1302 –1313, August 1995.
7. Price, W.W., Wirgau, K.A, Murdoch, A., Mitsche, J.V., Vaahedi, E., and El-Kady, M., "Load modeling for power flow and transient stability computer studies", *IEEE Transactions on Power Systems*, Vol. 3, No. 1, PP. 180 –187, February 1988.
8. Marti, J.R., Myers, T.O., "Phase-domain induction motor model for power system simulators", WESCANEX 95, IEEE Proceedings on Communications, Power, and Computing Conference, Vol. 2, PP. 276 –282 1995.
9. Reliability Test System Task Force, "IEEE Reliability Test System", *IEEE Transactions on Power Apparatus and Systems*, Vol. PAS-98, No. 6, pp 2047-2054, November/December 1979.

Biographies

A. P. Sakis Meliopoulos (M '76, SM '83, F '93) was born in Katerini, Greece, in 1949. He received the M.E. and EE diploma from the National Technical University of Athens, Greece, in 1972 and the M.S.E.E. and PH.D degrees from the Georgia Institute of Technology in 1974 and 1976, respectively. In 1971, he worked for Western Electric in Atlanta, Georgia. In 1976 he joined the Faculty of Electrical Engineering, Georgia Institute of Technology, where he is presently a professor. He is active in teaching and research in the general modeling, analysis, and control of power systems. He has made significant contributions to power system grounding, harmonics, and reliability assessment of power systems. He is the author of the following: *Power Systems Grounding and Transients*, Marcel Dekker, June 1988, *Lightning and Overvoltage Protection*, Section 27, *Standard Handbook for Electrical Engineers*, McGraw

Hill, 1993, and the monograph, *Numerical Solution Methods of Algebraic Equations*, EPRI monograph series. Dr. Meliopoulos is a member of the Hellenic Society of Professional Engineering and the Sigma Xi.

Sun Wook Kang (M '99) was born in Chonju, South Korea in 1970. He received the B.S. in 1997 from Chonbuk National University, Chonju, South Korea, the M.S.E.E. and Ph.D. in 1999 and 2001 from Georgia Institute of Technology. He is currently a post-doctoral fellow at Georgia Institute of Technology. His research interest is in the power system security, reliability, and planning.

George J. Cokkinides (M '85) was born in Athens, Greece in 1955. He obtained the B.S., M.S., and Ph.D. degree at the Georgia Institute of Technology in 1978, 1980, and 1985, respectively. From 1983 to 1985, he was a research engineer at the Georgia Tech Research Institute. Since 1985, he has been with the university of South Carolina where he is presently an Associate Professor of Electrical Engineering. His research interests include power system modeling and simulation, power electronics applications, power system harmonics, and measurement instrumentation. Dr. Cokkinides is a member of the IEEE/PES and the Sigma Xi.

Roger A. Dougal earned the Ph.D. degree in electrical engineering at Texas Tech University in 1983, then joined the faculty at the University of South Carolina. Dr. Dougal has received the *Samuel Litman Distinguished Professor of Engineering* award, has been honored as a *Carolina Research Professor*, and is a Senior Member of the IEEE. His current research interests include power electronics, electrochemical power sources, and modeling and simulation tools for interdisciplinary dynamic systems. Prof. Dougal is the director of the Virtual Test Bed project, which is developing an advanced simulation and virtual prototyping capability for multidisciplinary dynamic systems.